Lattice Gas Model for CO Electrooxidation on Pt−Ru Bimetallic Surfaces

M. T. M. Koper,*,† J. J. Lukkien,‡ A. P. J. Jansen,† and R. A. van Santen†

Laboratory of Inorganic Chemistry and Catalysis, Schuit Institute of Catalysis, and Department of Mathematics and Computing Science, Eindhoven University of Technology, 5600 MB Eindhoven, The Netherlands

Received: February 11, 1999

We propose a lattice gas model for the carbon monoxide oxidation on platinum−ruthenium electrode surfaces. The kinetic model includes the main mechanistic "bifunctional" features as they are generally agreed upon in the literature. The CO stripping voltammetry is solved by dynamic Monte Carlo simulations. For a randomly dispersed alloy of Ru and Pt, the model gives a satisfactory semiquantitative agreement with the experimental CO stripping results of Gasteiger et al. [*J. Phys. Chem.* **1994**, *98*, 617]. It is shown how the bifunctional mechanism cannot operate if CO is not mobile on the surface, and a simple Tafel-type experiment with a low concentration of active Pt−Ru sites is suggested to check quantitatively the CO mobility rate. On a surface with large Ru islands, the overpotential for CO oxidation increases, and two CO stripping peaks may appear if the CO mobility is sufficiently low. A mean-field model of the system reproduces the DMC results for high CO mobility but breaks down for a system with large Ru islands and a comparatively low CO surface diffusion constant.

1. Introduction

Platinum−ruthenium electrodes are considered to be the most active electrocatalysts for the oxidation of small organic molecules and find practical application in low-temperature fuel cells. Their enhanced activity with respect to the pure elements is explained by the so-called bifunctional mechanism, in which the Ru sites act as nucleation centers for the oxygen-containing species that are necessary for removing the poisonous carbon monoxide from the Pt sites (for two recent reviews, see refs 1 and 2). Due to its practical importance, there has been a wealth of experimental studies on Pt−Ru electrodes for the electrooxidation of carbon monoxide, methanol and formic acid.[3−14] Especially the recent work of Gasteiger et al.[4−7] deserves to be mentioned. These authors have carried out detailed studies on Pt−Ru alloy electrode surfaces that were carefully prepared and well characterized by UHV techniques before their transfer to the electrochemical cell. In this way, they were able to obtain reliable data on the electrocatalytic activity as a function of the Ru content of the electrode surface, for CO, methanol, and formic acid.

Even though the mechanism of CO oxidation on Pt−Ru electrodes appears to be relatively well understood, the generally accepted bifunctional mechanism is based on a few implicitly made assumptions. The appropriateness of these assumptions, together with the question of whether they really lead to the observed experimental behavior, can only be tested convincingly by quantitative theoretical modeling. Apart from giving a more satisfying rationale behind the experimental data, theoretical modeling is also, we believe, an essential ingredient in a systematic search for improved electrocatalysts.

Theoretical simulation can be approached in two different ways. On the one hand, one can start from the quantum-chemical point-of-view[15] and calculate the affinity of various alloy surfaces, as modeled by small clusters, for the CO oxidation reaction. This approach has been followed recently, in the context of electrocatalysis, by Anderson and co-workers[17,18] using their semiempirical ASED-MO method.

In this paper, however, we start from the other direction, which takes the statistical-mechanical point-of-view. In this approach, one addresses issues such as the role of CO mobility, the distribution of Ru on the surface (homogeneous, inhomogeneous, random, ordered, ...) and the relative rates of the different reactions on the electrochemical activity of the electrode, by employing a lattice gas model. The rate parameters entering such a model are chosen such that the experimental data are mimicked as closely as possible (and as is useful within the context of a simple model). Eventually, and ideally, one would like to obtain these rate parameters from quantum-chemical calculations,[15,16] but at the present time this is not feasible for catalytic reactions at the electrified metal−water interface.

The lattice gas model we suggest in this paper is a natural extension of a simple model we recently proposed for the CO oxidation on a platinum electrode.[19] In that paper we also introduced an efficient dynamic Monte Carlo (DMC) method to calculate cyclic voltammograms and chronoamperometric transients without making any further approximations in the statistical-mechanical treatment of the adsorbate configurations. (For two other recent Monte Carlo simulation studies of CO electrooxidation, see refs 20 and 21.) The DMC simulations will be compared to an effective mean-field model in which the various adsorbate coverages are assumed to be homogeneously distributed.

The purpose of this paper is therefore to present a simple kinetic model that includes all the important ingredients that are commonly believed to govern the CO oxidation on Pt−Ru electrodes. Our goal is to test the microscopic model in relation to the experimental data and to suggest new experiments that specifically address certain assumptions that have to be made in order to obtain qualitative or semiquantitative agreement with experiment.

† Schuit Institute of Catalysis.
‡ Eindhoven University of Technology.

10.1021/jp990520k CCC: $18.00
Published on Web 06/15/1999

The remainder of this paper is organized as follows. In section 2 we present the reaction model and the computational details of our DMC simulations. In section 3 we analyze the linear sweep CO stripping voltammetry under a variety of conditions, with the main aim to assess the role of CO surface mobility and the Ru distribution (random, islands, ordered) on the electrocatalytic activity. Section 4 summarizes our results and discusses the possibilities for future experimental and theoretical research.

2. Model

In our model, we consider a square lattice of surface sites. A site can either be a Pt atom or a Ru atom. We do not expect any differences between a square or triangular lattice of sites as long as a random distribution of Ru and Pt is considered and as long as lateral interactions between the adsorbates are neglected. Although lateral interactions between CO and coadsorbed water are presumably quite important in understanding certain voltammetric features of CO oxidation on Pt single crystal surfaces,[21] in this work we will ignore the lateral interactions in order not to distract too much from the catalytic properties of the alloy surfaces per se. CO is adsorbed onto the Pt−Ru surface until 99% of all sites is occupied. This coverage of 0.99 is considered as the saturation coverage. CO is adsorbed with equal probability on Pt and Ru sites, which is corroborated by the experimental fact that CO saturation coverages on bare Pt and Ru electrodes are very similar.[5] We will study the stripping of the adsorbed CO in a single linear sweep voltammogram, as there are some good data on this type of experiment available in the paper of Gasteiger et al. CO is assumed to be oxidized from the surface by reacting with an adsorbed OH species, which in acidic solutions results from the dissociative water adsorption (a detailed discussion of the model can be found in ref 19). Hydroxyl can be formed on both the Ru and the Pt sites:

$$H_2O + *_{Ru} \rightleftharpoons OH_{Ru} + H^+ + e^- \quad (2.1)$$

$$H_2O + *_{Pt} \rightleftharpoons OH_{Pt} + H^+ + e^- \quad (2.2)$$

CO can react with a neighboring OH in four different ways:

$$CO_{Ru} + OH_{Ru} \rightarrow CO_2 + H^+ + 2*_{Ru} + e^- \quad (2.3)$$

$$CO_{Ru} + OH_{Pt} \rightarrow CO_2 + H^+ + *_{Ru} + e^- \quad (2.4)$$

$$CO_{Pt} + OH_{Pt} \rightarrow CO_2 + H^+ + 2*_{Pt} + e^- \quad (2.5)$$

$$CO_{Pt} + OH_{Ru} \rightarrow CO_2 + H^+ + *_{Pt} + *_{Ru} + e^- \quad (2.6)$$

One of the reasons for the high overpotential of the CO oxidation on Pt electrodes is the relative difficulty with which OH is formed on Pt. The essential feature of the bifunctional mechanism lies in the fact that OH forms more easily on the more oxyphilic Ru, and this makes it possible that CO adsorbed on Pt sites can react with an OH adsorbed on a neighboring Ru site through reaction 2.6. It will be shown below that this can indeed lead to an enhanced catalytic activity of the Pt−Ru alloy with respect to the bare Pt and Ru electrodes, provided that the intrinsic rate constant for reaction 2.6, k_6, is higher than that of reaction 2.3, k_3, and provided that CO can easily diffuse over the surface.

In our model simulations, we have to specify the rates of reactions 2.1−2.6, as well as the rate with which an adsorbed CO can exchange places with an empty site (or, more realistically, with a physisorbed water molecule):

$$CO_{Pt,Ru} + *_{Pt,Ru} \rightarrow *_{Pt,Ru} + CO_{Pt,Ru} \quad (2.7)$$

The rate constant for this process is D s^{-1}, corresponding to a surface diffusion coefficient of ca. $D \times 10^{-15}$ cm^2 s^{-1}, and for simplicity we assume it to have one constant value, regardless of whether CO or the empty site is on Pt or Ru. A D equal to 1000 corresponds to a root-mean-square displacement of ca. 45 sites/s. The other rates are assumed to obey the Butler−Volmer law for electrochemical reactions and are given by

TABLE 1: Rate Constants in s^{-1}

k_1^0	0.2	k_3^0	0.1
k_{-1}^0	10^4	k_4^0	0.1
k_2^0	40	k_5^0	1
k_{-2}^0	5	k_6^0	1

$$k_{OH,ads}^{Ru} = k_1 = k_1^0 \exp(\alpha_1 e_0 E/k_B T) \quad (2.8)$$

$$k_{OH,des}^{Ru} = k_{-1} = k_{-1}^0 \exp(-(1-\alpha_1) e_0 E/k_B T) \quad (2.9)$$

$$k_{OH,ads}^{Pt} = k_2 = k_2^0 \exp(\alpha_2 e_0 E/k_B T) \quad (2.10)$$

$$k_{OH,des}^{Pt} = k_{-2} = k_{-2}^0 \exp(-(1-\alpha_2) e_0 E/k_B T) \quad (2.11)$$

$$k_{CO_2,des}^{Ru} = k_3 = k_3^0 \exp(\alpha_3 e_0 E/k_B T) \quad (2.12)$$

$$k_{CO_2,des}^{RuPt} = k_4 = k_4^0 \exp(\alpha_4 e_0 E/k_B T) \quad (2.13)$$

$$k_{CO_2,des}^{Pt} = k_5 = k_5^0 \exp(\alpha_5 e_0 E/k_B T) \quad (2.14)$$

$$k_{CO_2,des}^{PtRu} = k_6 = k_6^0 \exp(\alpha_6 e_0 E/k_B T) \quad (2.15)$$

where the α's are the transfer coefficients (taken as 0.5 in all that follows), E is the electrode potential, and e_0, k_B, and T have their usual meanings. We will refer to the k_j^0 as the "intrinsic" rate constants, and they include the proton and water concentrations at the surface (when applicable), which are both assumed to be constant. All reaction rate constants are assumed to be independent of the Ru/Pt ratio of the surface, and have the dimension s^{-1}. The total current density i due to these reactions is given by Faraday's law

$$i = e_0(\upsilon_1 - \upsilon_{-1} + \upsilon_2 - \upsilon_{-2} + \upsilon_3 + \upsilon_4 + \upsilon_5 + \upsilon_6) \quad (2.16)$$

where υ_j denotes the rate of the jth reaction (in cm^{-2} s^{-1}). These rates are calculated by the DMC method described in detail in refs 19 and 22 and are obtained from

$$\upsilon_j = \frac{N_j}{a^2 L^2 \Delta t} \quad (2.17)$$

where N_j is the number of times that reaction j has occurred in the time step Δt, a is the lattice constant (taken as 2.75 Å, corresponding to 1.32×10^{15} sites/cm^2), and L^2 is the size of the square lattice in the simulation (128×128 in all simulations reported below). The temperature in all our simulations has been fixed at 300 K.

3. Results and Discussion

3.1. Choice of Rate Parameters. The intrinsic rate constants in our simulations were fixed at the values given in Table 1. It

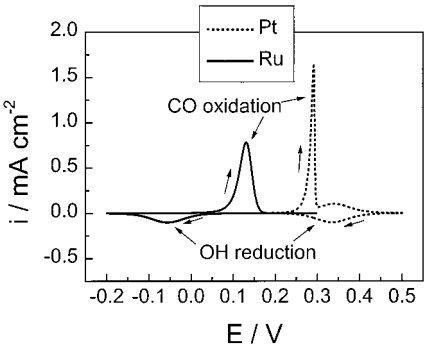

Figure 1. CO stripping voltammetry on Pt and Ru for a 0.99 monolayer of CO in the mean-field approximation. Rate constants as in Table 1; scan rate $\upsilon = 50$ mV/s.

is important to discuss the rationale behind these choices. First, we chose values for the rate constants k_1^0, k_{-1}^0 and k_3^0, and k_2^0, k_{-2}^0, and k_4^0 to give a reasonable representation of the CO stripping voltammetry on the pure Ru and Pt electrodes, respectively. The rate constants for Pt are similar to the "FAST" rate constants used in our previous paper,[19] which were argued to give a fair description of some of the essential features of the CO stripping voltammetry on Pt. "FAST" in this respect means that the CO + OH intrinsic reaction rate constant is high in the sense that the CO oxidation peak for Pt occurs before the electrode is fully occupied by OH in the blank cyclic voltammogram. For Ru, the situation is rather different, as the CO oxidation peak occurs in a potential region where in the blank cyclic voltammogram the electrode is already covered by oxygenated species. This implies a relatively low rate constant of the CO + OH reaction, a situation dubbed "SLOW" in our previous paper. The rate constants for OH adsorption and desorption were chosen such that their cyclic voltammetry appears reversible at 50 mV/s, but with the difference that at Ru the oxidation and reduction waves occur at much lower potentials (basically, this corresponds to a more negative equilibrium potential for the OH formation on Ru). The CO mean-field stripping voltammograms for Ru and Pt, which apply in the case of high CO surface mobility, are compared in Figure l, and we note that our model voltammograms reproduce the following essential experimental facts:

• The CO oxidation peak on Ru occurs at a potential ca. 0.16 V less positive than on Pt; experimentally, Gasteiger et al.[5] reported a difference in peak potentials of ca. 0.14 V.

• Experimentally, the reduction peak of the oxygenated species during the negative-going return scan occurs at a potential ca. 0.5 V less positive on Ru than on Pt. In our model, the difference between the OH reduction peaks is ca. 0.4 V. At any rate, this difference is larger than the difference between the CO oxidation peaks, which is a result of the fact that CO oxidation is "FAST" on Pt and "SLOW" on Ru.

• The CO oxidation peak is relatively sharp on Pt, and broad on Ru, in agreement with experiment. Again, this is due to the FAST/SLOW properties. We remark that the model stripping peaks are still much sharper and hence of higher current than the experimental stripping peaks on the polycrystalline surfaces. This is due to the fact that in our model the pure Pt and Ru surfaces are perfectly homogeneous and there are no lateral interactions between the adsorbed CO molecules. Both surface heterogeneity and lateral interactions may broaden the stripping peak. The Pt peak, however, is rather similar to the sharp experimental CO stripping peak on Pt(100) and Pt(111) single crystal electrodes (see, e.g., Figure 1 in ref 5).

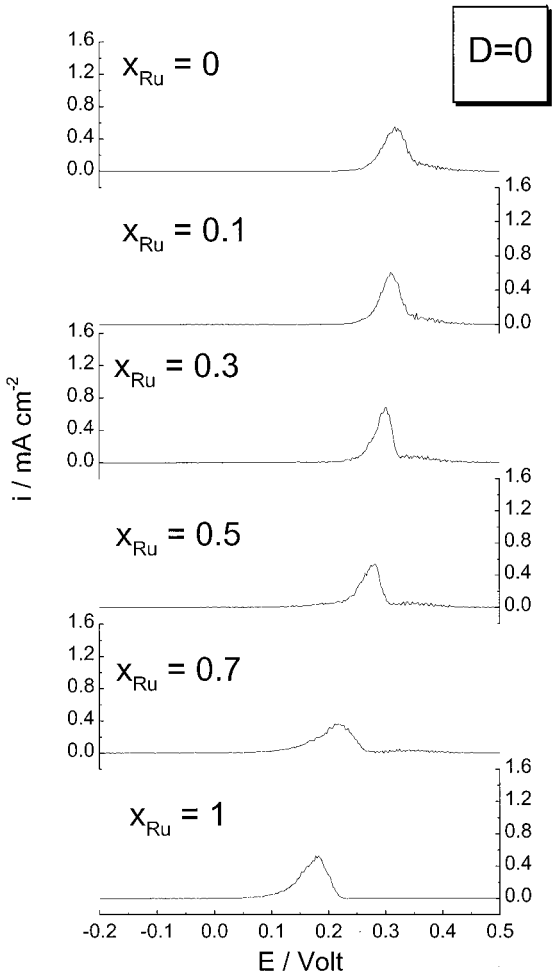

Figure 2. CO stripping voltammetry for pure Pt ($x_{Ru} = 0$), various Pt−Ru alloy surfaces, and pure Ru. Rate constants as in Table 1; $D = 0$, scan rate $\upsilon = 50$ mV/s.

• The intrinsic rate constant for CO oxidation on Pt is higher than that of Ru, i.e., $k_5^0 > k_3^0$. Gasteiger et al.[5] have reached such a conclusion from potential step experiments.

The rate constants for the CO + OH reactions on the Pt−Ru pairs were chosen as follows. In order to observe any catalytic enhancement at all, it is necessary that $k_6^0 > k_3^0$, as will be discussed below. In all our simulations we chose $k_6^0 = k_5^0$, which gives good agreement with experiment. In order to have a meaningful voltammetry at low CO diffusion rates D, it was necessary to include reaction 2.4 as well, and we have put $k_4^0 = k_3^0$. It is noteworthy that reaction 2.4 plays no role in the model when the CO diffusion rate is high.

3.2. CO Stripping Voltammetry on Homogeneous Pt−Ru Electrode Surfaces. 3.2.1. DMC Simulations. In Figures 2−4 we compare the CO stripping voltammetry of homogeneous Pt−Ru electrodes with varying Ru fraction for three different CO diffusion rates at a scan rate of 50 mV/s. In Figure 2 $D = 0$, in Figure 3 $D = 1$, and in Figure 4 $D = 1000$. The peak potential is plotted vs the Ru surface composition for the three different diffusion rates in Figure 5. Of these plots, the one for $D = 1000$ compares most favorably with experiment. The peak shapes reported in Figure 4 for $D = 1000$ have some quite remarkable resemblances to the experimental stripping voltammograms of Gasteiger et al. (Figure 3 in ref 5). In agreement with experiment, the peak shape for low Ru content (10%) is broad and of low current and progressively sharpens for higher Ru fractions, whereas for pure Ru the peak is again quite broad.

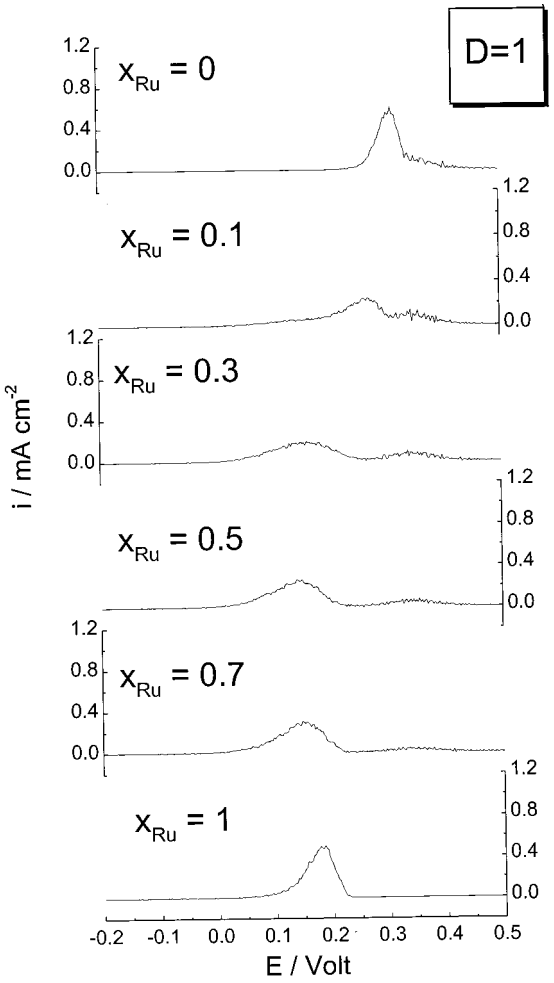

Figure 3. CO stripping voltammetry for pure Pt ($x_{Ru} = 0$), various Pt−Ru alloy surfaces, and pure Ru. Rate constants as in Table 1; $D = 1$, scan rate $\upsilon = 50$ mV/s.

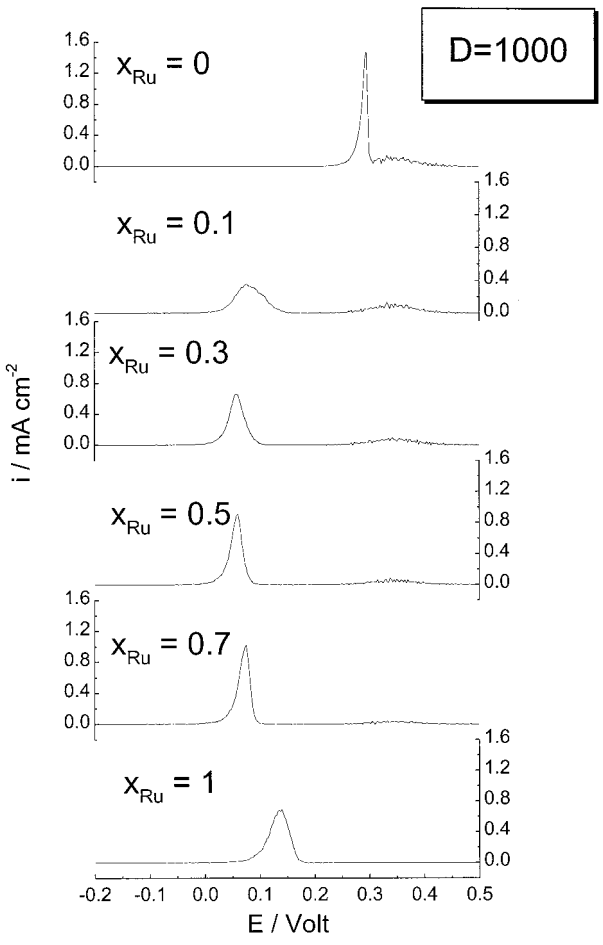

Figure 4. CO stripping voltammetry for pure Pt ($x_{Ru} = 0$), various Pt−Ru alloy surfaces, and pure Ru. Rate constants as in Table 1; $D = 1000$, scan rate $\upsilon = 50$ mV/s.

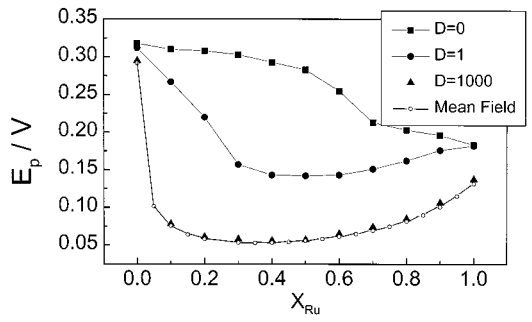

Figure 5. CO stripping peak potential, E_p, as a function of the Ru fraction x_{Ru}, for $D = 0$, $D = 1$, $D = 1000$, and the mean-field model given by eqs 3.1. Scan rate 50 mV/s.

It is instructive to remark that the broad peak for the low Ru fraction is *not* caused by the long diffusion path for CO to reach the active sites, as was suggested by Gasteiger et al.[5] If this were true, increasing D should make the peak sharper, which is not the case for this particular simulation as D is already quite high. The broad peak is the result of the low concentration of active sites, which leads to a lower effective CO oxidation rate. At the optimum composition, the shift in peak potential with respect to pure Ru is ca. 80 mV, in good agreement with experimental data of Gasteiger et al. This supports our choice for the rate constant k_6, the rate of the $CO_{Pt} + OH_{Ru}$ reaction. Also very nicely reproduced by our simulations is the fact that only a low fraction of Ru is needed to see a strong catalytic enhancement, i.e., a significantly lower CO stripping peak potential. A Ru fraction of only 10% lowers the peak potential by about 200 mV with respect to pure Pt, a number in good agreement with the experimental data. These results are strong evidence that CO must be mobile on these Pt−Ru surfaces. The plots for $D = 10$ and $D = 100$ are essentially similar to those for $D = 1000$.

Another interesting effect nicely illustrated by Figures 2 and 5 is the fact that for completely immobilized CO, the bifunctional mechanism does not work, not even on a well-mixed Pt−Ru surface. Increasing the value of k_6^0, the rate constant for the $CO_{Pt} + OH_{Ru}$ reaction, does not have any significant influence on the catalytic activity for $D = 0$.

The scan rate may have a pronounced effect of the shape of the E_p vs x_{Ru} plot as shown in Figure 6. For a low diffusion rate ($D = 1$), it is found that for the surfaces with a low Ru fraction, the peak potential may be "delayed" significantly if the scan rate is too high. For 50 mV/s, the diffusion of the CO to the active sites of the $x_{Ru} = 0.1$ surface is too slow to keep up with the relatively fast potential changes, and for the reaction to occur at the active sites CO surface diffusion becomes rate determining. If the scan rate is appropriately low (5 mV/s), CO has sufficient time to reach the active sites and reaction is rate limiting. For a high diffusion rate ($D = 1000$), no significant effect of the scan rate on the qualitative features of the E_p vs x_{Ru} plot is observed. Figure 6 suggests that it would be interesting to study the effect of a wider range of sweep rates on the CO stripping peak potential of a surface with a low Ru fraction. In Figure 7 we plot the peak potential E_p vs the logarithm of the scan rate υ, which is in fact equivalent to a

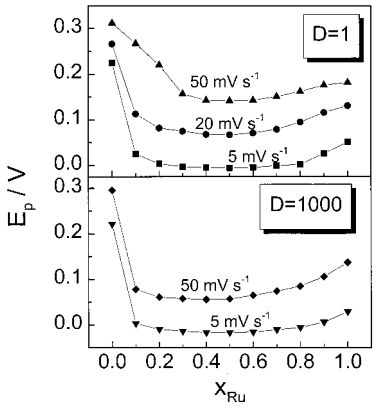

Figure 6. Scan rate dependence of the E_p-x_{Ru} plots for $D = 1$ and $D = 1000$.

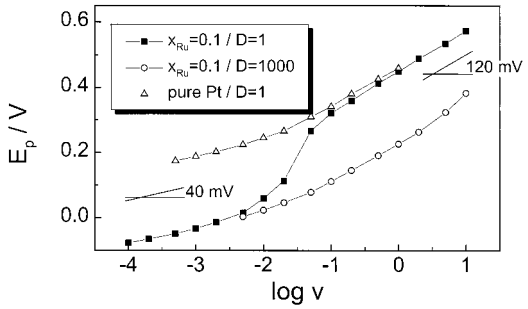

Figure 7. Tafel plots, E_p vs log(υ), for pure Pt ($D = 1$), $x_{Ru} = 0.1$ ($D = 1$), and $x_{Ru} = 0.1$ ($D = 1000$).

Tafel plot, for the $x_{Ru} = 0.1$ surface and pure Pt. As was discussed in detail in our previous paper,[19] our model predicts that on pure Pt the Tafel slope is 40 mV at low υ (or low potential), and 120 mV at high υ (or high potential), as a result of the two-step nature of the Langmuir−Hinshelwood mechanism, i.e., reactions 2.2 and 2.5. For the $x_{Ru} = 0.1$ surface and high CO surface mobility ($D = 1000$), a similar Tafel plot is obtained but is downshifted by ca. 220 mV, the amount by which the overpotential for CO oxidation is reduced for this surface. However, if diffusion is slow, something interesting is observed, as illustrated by the $D = 1$ curve in Figure 7. At low scan rates, CO has sufficient time to diffuse to the active sites and the peak potential is very similar to the $D = 1000$ curve. At higher scan rates, the low concentration of active sites makes it more difficult for the relatively immobile CO to reach the active sites and there is a delay in the peak potential with respect to the $D = 1000$ curve. At very high scan rates, most of the CO is oxidized at Pt instead of at the active Pt−Ru sites since diffusion is now much too slow to reach the active sites on the time scale of the potential variation. Hence the peak potential is very close to that for pure Pt (at the same D). This leads to the highly nonlinear Tafel plot shown in Figure 7. Note that the $D = 1000$ curve also begins to deviate from the expected 120 mV slope at $\upsilon = 10$ V/s, and it is no coincidence that this deviation starts at a scan rate 3 orders of magnitude higher than for the $D = 1$ curve. We believe that this experiment, i.e., the measurement of the CO stripping voltammetry at a wide range of scan rates for a surface with a low concentration of active Ru sites, could constitute a simple way to assess more quantitatively the role of CO mobility. Gasteiger et al.[5] have in fact carried out measurements at the three different scan rates considered in Figure 6. They observed that, for the 7% Ru surface, the shift in the peak potential is somewhat less for the 50 mV/s than for the 20 and 5 mV/s sweeps. Though we find it difficult to assess the experimental significance of this result,

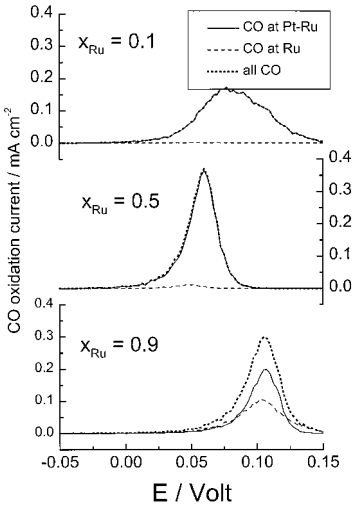

Figure 8. Contribution of the various CO oxidation pathways to the total CO oxidation current for the homogeneous $x_{Ru} = 0.1$, 0.5, and 0.9 surfaces. Scan rate 50 mV/s.

it could mean that although CO diffuses rather rapidly over the surface, it may still cause some rate limitations if the Ru concentration of the surface is low.

We mentioned before that the Pt−Ru surface is not more active than pure Ru if the rate constant k_6^0 is not greater than k_3^0. For $k_6^0 = k_3^0$, the peak potential is almost equal to that of the pure Ru surface, a logical result. We find that the higher the rate of reaction 2.6, the lower the peak potential, with a saturation value of ca. −0.10 V for an infinitely fast $CO_{Pt} + OH_{Ru}$ reaction, which is about a 0.15 V gain in activity compared to the rate constants given in Table 1.

For the simulations with high CO mobility, which seem to mimic most closely the experimental situation, almost all CO reacts through reaction 2.6. This is illustrated in Figure 8, in which we compare the rate of the various CO + OH reactions (2.3)−(2.6) for three different Ru fractions. For all surfaces, reaction 2.6 is dominant, apart from those with a Ru fraction close to 1. Figure 9 shows, for the 50% Ru surface, the coverages of CO and empty sites on Pt and Ru during the voltammetric scan. Note that CO disappears first from the Ru part of the surface and that the CO concentration on Pt initially increases because the CO is pushed from the Ru sites by the nucleating OH.

3.2.2. Mean-Field Model. It is interesting to compare the results for high D with an effective mean-field model in which we assume the CO to be distributed homogeneously on the Pt and Ru parts of the surface. In this model, there are four variables: the CO coverage of the Ru part of the surface, θ_{CO}^{Ru}, the CO coverage of the Pt part, θ_{CO}^{Pt}, the OH coverage of the Ru part, θ_{OH}^{Ru}, and the OH coverage of the Pt part, θ_{CO}^{Pt}. The general expression for the time evolution of these four coverages is

$$\frac{d\theta_A^i}{dt} = k_{ads,A}^i \theta_*^i - k_{des,A}^i \theta_A^i - 4k_{rx}^{ii} x_i \theta_A^i \theta_B^i - 4k_{rx}^{ii'}(1 - x_i)\theta_A^i \theta_B^{i'} - 4D_A(1 - x_i)\theta_A^i \theta_*^{i'} + 4D_A(1 - x_i)\theta_*^i \theta_A^{i'} \quad (3.1)$$

where if A = CO then B = OH, or the reverse, and if i = Pt then i′ = Ru, or the reverse, and θ_*^i is the average coverage of empty sites on metal i. Adsorption, desorption, and reaction rate

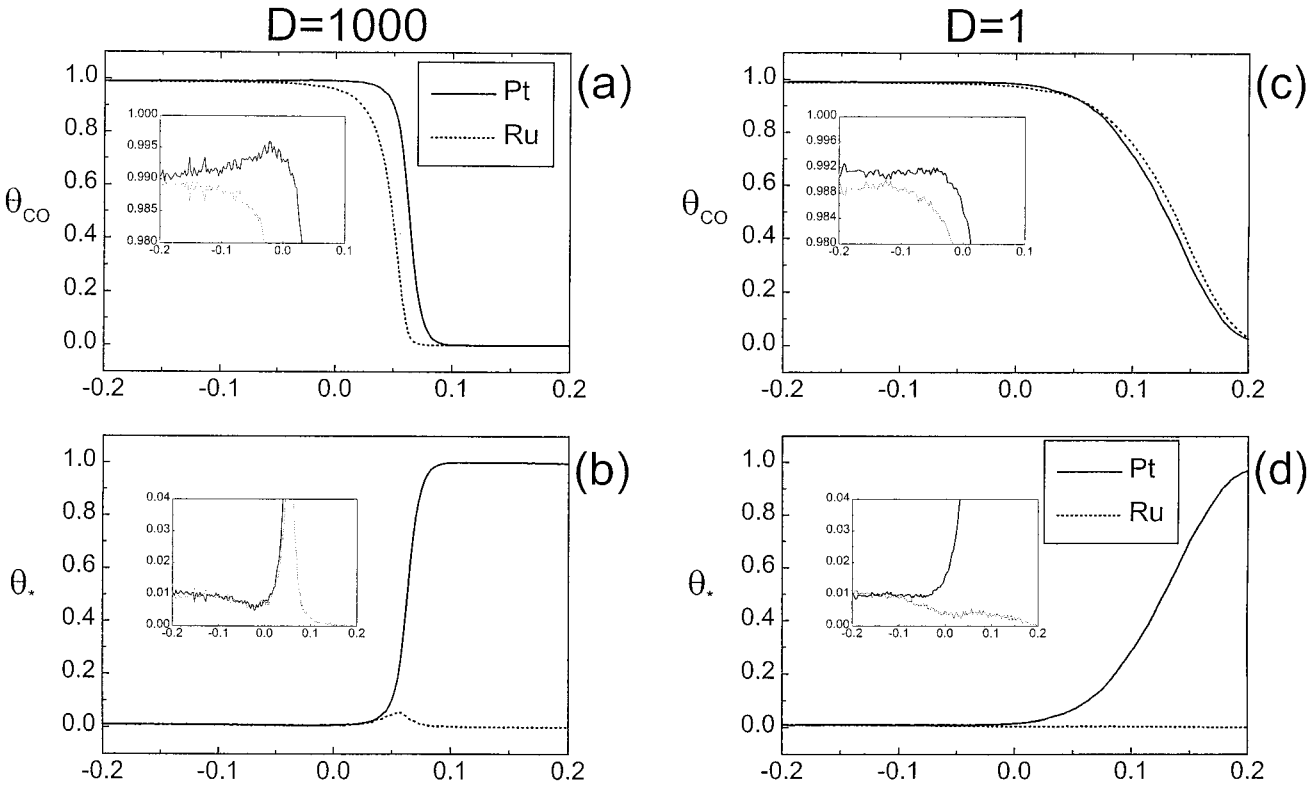

Figure 9. Average CO and empty site concentrations θ_{CO} and θ_* on Pt and Ru for fast and slow CO diffusion on a random $x_{Ru} = 0.5$ surface: (a) θ_{CO} for $D = 1000$; (b) θ_* for $D = 1000$; (c) θ_{CO} for $D = 1$; (d) θ_* for $D = 1$. Scan rate 50 mV/s. The insets in all four figures zoom in on the evolution of the various coverages at the beginning of the sweep.

constants, k_{ads}, k_{des}, k_{rx}, correspond to those given in the model section. Note that the terms for the diffusion hops from Pt to Pt or from Ru to Ru cancel. The linear sweep voltammogram for this mean-field model is obtained by solving these equations numerically by standard integration routines. The peak potentials predicted by the mean-field model are compared with the DMC results in Figure 5. We find that the mean-field model gives a good description of the DMC results over the entire x_{Ru} range. Mean field also predicts the optimum Ru fraction to be smaller than 0.5; for 50 mV/s it is ca. 0.35. However, this seems to be mainly a scan rate effect. For 1 mV/s, for which mean field is computationally a lot cheaper than DMC, we find that the optimum fraction is very close to 0.5.

3.3. CO Stripping Voltammetry on Inhomogeneous and Ordered Pt−Ru Electrode Surfaces. 3.3.1. DMC Simulations. In experimental practice, it is difficult to prepare a homogeneous Pt−Ru electrode surface, and to keep it that way. Most of the experiments in the literature involved, or are most likely to have involved (since no structural characterization of the surface was done), a surface on which Ru was segregated into islands. Friedrich et al.[10] have shown by STM that Ru electrodeposited onto Pt(111) single crystal electrodes forms small 3−4 nm islands. Gasteiger et al.[5] have shown that alloy surfaces that exhibit small Ru segregates instead of an atomically dispersed structure are catalytically less active and resemble more closely a linear superposition of the voltammetric features of the pure elements. On the other hand, the homogeneous surface is not necessarily the most active one. Since the bifunctional mechanism generally works best if the number of PtRu pairs is maximized, theoretically, an ordered surface in which Ru is distributed in the Pt surface in a chessboard structure should be the catalytically most active one (that is, for a square lattice). In this section, we will compare the CO stripping voltammetry on Pt−Ru surfaces with large Ru islands, smaller Ru islands, a homogeneous random mixture of Ru, and an ordered chessboard structure of Pt−Ru, all at $x_{Ru} = 0.5$. The three nonordered surfaces used in our simulations are shown in Figure 10. The scale in the figure assumes a lattice constant of 2.75 Å.

Figure 11 compares the voltammograms of the four surfaces for high CO mobility $D = 1000$. The ordered surface is indeed seen to be the most active, although the gain is only a 20 mV in peak potential with respect to the randomly mixed Pt−Ru surface. For the surface with large islands, the shift in peak potential is only ca. 20 mV with respect to a pure Ru surface, so such surfaces really present a significant loss in catalytic activity with respect to the homogeneous surfaces at the same overall composition. However, for these high CO mobility rates, the voltammetric curves do not resemble a linear superposition of the voltammetric features of the pure elements. Such behavior is only observed for low D, as is illustrated in Figure 12, which shows the CO stripping voltammetry on the surface with large Ru islands for various diffusion rates. For $D = 10$ one observes, for this particular surface, the splitting of the CO oxidation peak into two peaks, one for CO on Pt−Ru and Ru and one for CO on Pt, and for $D = 0$ the respective peak potentials are indeed very close to those for the pure surfaces. The second peak, that for CO on Pt, is in fact at a slightly lower potential than for pure Pt because the CO from the Pt−Ru edges has already reacted through reaction 2.6, creating more free sites for OH_{Pt} formation, which lowers the peak potential.

3.3.2. Mean-Field Model. We can modify our mean-field model to account for the existence of islands by specifying explicitly in the model the relative number of Pt−Pt, Ru−Ru, and Pt−Ru neighbors, denoted ⟨Pt,Pt⟩, ⟨Ru,Ru⟩, and ⟨Pt,Ru⟩, respectively. Table 2 gives these concentrations for the three

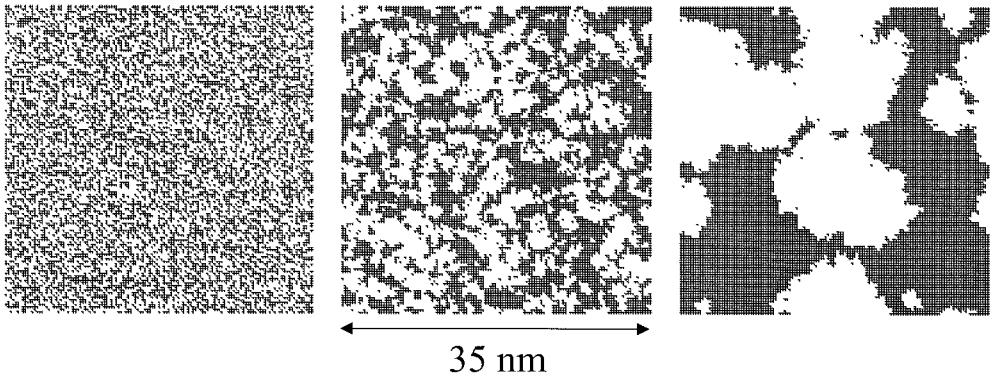

Figure 10. Three different nonordered surfaces used for the simulations in Figure 11. Black is Pt, white Ru.

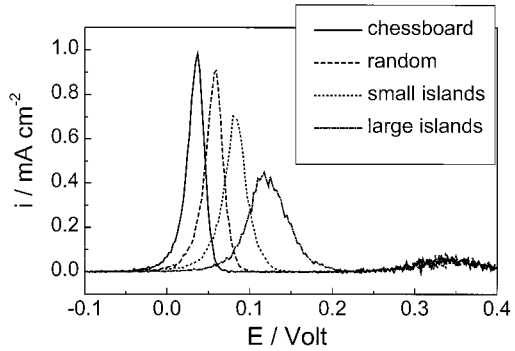

Figure 11. Comparison of the CO stripping voltammetry for the four different surfaces described in the text (and shown in Figure 10). Scan rate 50 mV/s. D = 1000.

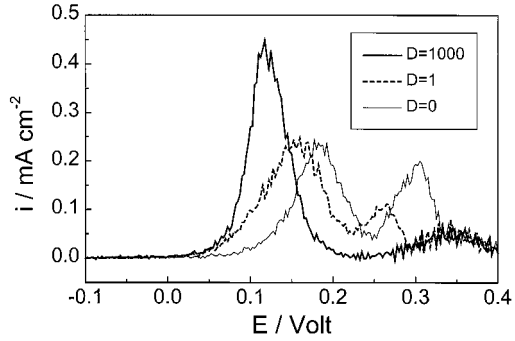

Figure 12. 2. Dependence of the CO stripping voltammetry for a x_{Ru} = 0.5 surface with large islands on the CO mobility *D*. Scan rate 50 mV/s.

TABLE 2: Neighbor Distributions of the Three Surfaces in Figure 10

	random	small islands	large islands
x_{Ru}	0.4985	0.4988	0.5177
⟨Pt,Pt⟩	0.2495	0.3910	0.4570
⟨Ru,Ru⟩	0.2465	0.3885	0.4923
⟨Pt,Ru⟩	0.5040	0.2205	0.0507

different surfaces shown in Figure 10. Note that ⟨Pt,Pt⟩ + ⟨Ru,Ru⟩ + ⟨Pt,Ru⟩ = 1. Equation 3.1 now becomes

$$\frac{d\theta_A^i}{dt} = k_{ads,A}^i \theta_*^i - k_{des,A}^i \theta_A^i - 4k_{rx}^{ii} P(i|i)\theta_A^i \theta_B^i - 4k_{rx}^{ii'} P(i'|i)\theta_A^i \theta_B^{i'} - 4D_A P(i'|i)\theta_A^i \theta_*^{i'} + 4D_A P(i'|i)\theta_*^i \theta_A^{i'} \quad (3.2)$$

where $P(i'|i)$ is the conditional probability that a site of type i′ neighbors a site of type site i. These probabilities are related to

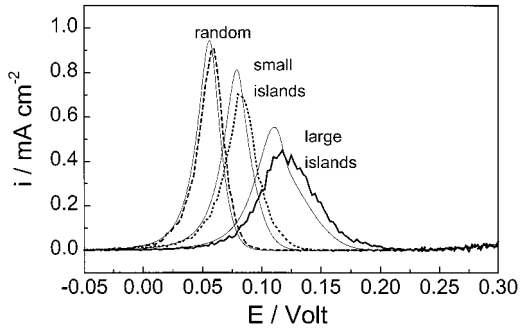

Figure 13. 3. Comparison of the DMC simulations and the mean-field model predictions for the CO stripping voltammetry as in Figure 11.

the *total* neighbor concentrations ⟨i′, i⟩ by the following equations

$$\langle i, i\rangle = x_i P(i|i)$$

$$\langle i', i\rangle = x_i P(i'|i) + (1 - x_i) P(i|i')$$

$$1 = P(i'|i) + P(i|i)$$

or

$$P(i|i) = \frac{\langle i, i\rangle}{x_i}$$

$$P(i'|i) = \frac{\langle i, i'\rangle - (1 - x_i) + \langle i', i'\rangle}{x_i}$$

Figure 13 compares the mean-field results to the DMC simulations. It is seen that the agreement is quite good, although for surfaces with larger islands there are larger differences than for the surface with a dispersed structure. Clearly, the mean-field model cannot describe the splitting of the CO oxidation peak for low *D* (Figure 12); in the mean-field model CO adsorbed on Pt will always preferentially react at the Pt−Ru active sites, because of the perfect mixing on the Pt part of the surface.

4. Summary and Conclusion

In this paper, we have presented a simple lattice gas model for the CO electrooxidation on Pt−Ru surfaces and solved the linear sweep stripping voltammetry by dynamic Monte Carlo simulations. Our model is based on the bifunctional mechanism originally proposed for this reaction by Watanabe and Motoo,[3] and commonly accepted by most workers in the field, and aims at giving a reasonable semiquantitative modeling of the experimental cyclic voltammetry data of Gasteiger et al.[5] Even though

the model may be very simple, since lateral interactions between adsorbates and the varying electronic properties of the surface were completely ignored, we believe that the model includes the main features that are currently believed to be governing the CO oxidation on Pt−Ru electrodes. We summarize our main conclusions.

- CO mobility is vital for the Pt−Ru surface to be electrocatalytically more active than the pure elements Pt and Ru. Comparison of our simulations with experiment suggests that CO is quite mobile. In the absence of CO mobility, the surface does not show any electrocatalytic enhancement with respect to pure Pt or Ru, even if Ru and Pt sites are well mixed. Our simulations suggest that a relatively straightforward way to assess the importance of CO mobility is to study the scan rate dependence of the CO stripping voltammetry on a surface with a low concentration of active Ru sites (Figure 7). For low scan rates one expects a clear enhancement with respect to pure Pt as the CO has sufficient time to reach the active sites, whereas at high scan rates the stripping peak should be quite similar to pure Pt as most of the CO will be oxidized from Pt rather than from the Pt−Ru active sites. Friedrich et al.[14] have recently estimated a lower limit for the CO surface diffusion coefficient on a Pt(111) covered by Ru islands and suggested $D_{CO} \geq 4\ 10^{-14}$ cm^2 s^{-1}, which corresponds to our $D \geq 50$ s^{-1}.
- The intrinsic rate constant for the $CO_{Pt} + OH_{Ru}$ reaction must be higher than the rate constant of the $CO_{Ru} + OH_{Ru}$ reaction for the surface to show any enhanced activity. Our simulations suggest that the intrinsic rate constant for the $CO_{Pt} + OH_{Ru}$ reaction is similar to that of the $CO_{Pt} + OH_{Pt}$ reaction.
- Both the qualitative features of the voltammetric peak shapes and the peak potential as a function of the Ru fraction of the surface compare favorably with the experiments of Gasteiger et al. Especially the experimentally observed fact that only a small Ru fraction is needed to effect a substantial enhancement in catalytic activity is reproduced nicely by the simulations.
- Multiple CO stripping peaks may occur if Ru islands on the surface are large and the CO mobility is comparatively low. Also, the catalytic activity, in terms of the CO stripping potential, is significantly lower for a surface with Ru islands than for a surface with a random Ru distribution, at the same overall surface fraction. Most active, at 50% Ru, is a surface with a chessboard Pt−Ru structure, although the catalytic enhancement with respect to the randomly distributed Ru is quite small.
- A mean-field model of the system, which assumes a homogeneous concentration of CO and OH on the Pt and Ru parts of the surface, reproduces the DMC simulations for high CO mobility quite well. For surfaces with large Ru islands, the agreement between mean-field and DMC gets less favorable. Mean-field modeling cannot reproduce the peak splitting that is observed for surfaces with large Ru islands and low CO mobility.
- As a more general point, we hope to have convinced the reader of the usefulness of DMC simulations in obtaining a better understanding of electrocatalytic systems. Clearly, we are not yet at the point where it is useful or even feasible to model electrocatalytic systems in quantitative detail. However, for a system like the one described in this paper, where some of the main effects seem to be qualitative rather than quantitative, kinetic model simulations can be a powerful tool in building a microscopic picture of what is going on, and in suggesting new experiments to assess more specifically the role of active site distribution and reactant surface mobility.

Acknowledgment. The research of M.T.M.K. was supported by a fellowship from the Royal Netherlands Academy of Arts and Sciences (KNAW).

References and Notes

(1) Ross, P. N., Jr. In *Electrocatalysis*; Lipkowski, J., Ross, P. N., Eds.; Wiley-VCH: New York, 1998; p 43.

(2) Jarvi, T. D.; Stuve, E. M. In *Electrocatalysis*; Lipkowski, J., Ross, P. N., Eds.; Wiley-VCH: New York, 1998; p 75.

(3) Watanabe, M.; Motoo, S. *J. Electroanal. Chem.* **1975**, *60*, 267.

(4) Gasteiger, H. A.; Markovic, N.; Ross, P. N., Jr.; Cairns, E. J. *J. Phys. Chem.* **1993**, *97*, 12020.

(5) Gasteiger, H. A.; Markovic, N.; Ross, P. N., Jr.; Cairns, E. J. *J. Phys. Chem.* **1994**, *98*, 617.

(6) Gasteiger, H. A.; Markovic, N.; Ross, P. N., Jr.; Cairns, E. J. *J. Electrochem. Soc.* **1994**, *141*, 1795.

(7) Markovic, N.; Gasteiger, H. A.; Ross, P. N., Jr.; Jiang, X.; Villegas, I.; Weaver, M. J. *Electrochim. Acta* **1995**, *40*, 91.

(8) Ianniello, R.; Schmidt, V. M.; Stimming, U.; Stumper, J.; Wallau, A. *Electrochim. Acta* **1994**, *39*, 1863.

(9) Frelink, T.; Visscher, W.; van Veen, J. A. R. *Electrochim. Acta* **1995**, *39*, 1871.

(10) Friedrich, K.; Geyzers, K.-P.; Linke, U.; Stimming, U.; Stumper, J. *J. Electroanal. Chem.* **1996**, *402*, 123.

(11) Kabbabi, A.; Faure, R.; Durand, R.; Beden, B.; Hahn, F.; Leger, J.-M.; Lamy, C. *J. Electroanal. Chem.* **1998**, *444*, 41.

(12) Chrzanowski, W.; Wieckowski, A. *Langmuir* **1998**, *14*, 1967.

(13) Davies, J. C.; Hayden, B. E.; Pegg, D. J. *Electrochim. Acta* **1998**, *44*, 1181.

(14) Friedrich, K. A.; Geyzers, K.-P.; Marmann, A.; Stimming, U.; Vogel, R. *Z. Phys. Chem.* **1999**, *208*, 137.

(15) van Santen, R. A.; Neurock, M. *Catal. Rev.-Sci. Eng.* **1995**, *37*, 557.

(16) Neurock, M.; Hansen, E. W. *Comput. Chem. Eng.* **1998**, *22*, S1045.

(17) Anderson, A. B.; Grantscharova, E. *J. Phys. Chem.* **1995**, *99*, 9149.

(18) Anderson, A. B.; Grantscharova, E.; Seong, S. *J. Electrochem. Soc.* **1996**, *143*, 2075.

(19) Koper, M. T. M.; Jansen, A. P. J.; van Santen, R. A.; Lukkien, J. J.; Hilbers, P. A. J. *J. Chem. Phys.* **1998**, *109*, 6051.

(20) Pethukov, A.; Akemann, W.; Friedrich, K. A.; Stimming, U. *Surf. Sci.* **1998**, *402*−*404*, 182.

(21) Orts, J. M.; Louis, E.; Sander, L. M.; Feliu, J. M.; Aldaz, A.; Clavilier, J. *Surf. Sci.* **1998**, *416*, 371.

(22) Lukkien, J. J.; Segers, J. P. L.; Hilbers, P. A. J.; Gelten, R. J.; Jansen, A. P. J. *Phys. Rev. E* **1998**, *58*, 2598.